Effect of Die Design on Die Drool Phenomenon for Metallocene Based LLDPE: Theoretical and Experimental Investigation

Kateřina Chaloupková, Martin Zatloukal

Polymer Centre, Tomas Bata University in Zlin, TGM 275, 762 72 Zlin, Czech Republic

Received 20 August 2007; accepted 9 August 2008
DOI 10.1002/app.29146
Published online 30 October 2008 in Wiley InterScience (www.interscience.wiley.com).

ABSTRACT: The effect of die design on the die drool phenomenon was investigated for metallocene based LLDPE. It has been found that die exit opening and the flared die design can significantly reduce the die drool phenomenon. Moreover, theoretical research has revealed that die drool onset can be explained by the negative/non-monotonic pressure profile generated inside the die and/or at the die exit region. © 2008 Wiley Periodicals, Inc. J Appl Polym Sci 111: 1728–1737, 2009

Key words: die drool; negative pressure; FEM modeling

INTRODUCTION

Die drool is a phenomenon occurring in melt extrusion of polyolefins, PVC, and filled polymers, which manifests itself as an undesirable build-up of material, normally on the lip or open face of extrusion dies. In commercial extrusion processes, die deposit can have a significant influence on the productivity, as it requires shutting down the processing line periodically to clean the die. Furthermore, die deposit can also affect the quality of the extruded product. This phenomenon has been extensively studied both theoretically as well as experimentally.[1–7] Recently, this phenomenon has been investigated experimentally for mLLDPE Exact 0201 (Exxon) at different processing conditions (mass flow rate and die exit temperature were varied).[7] Consequently, these experimental data were followed by viscoelastic FE calculations with the aim to find out simple to use criteria for detection of the die drool phenomenon. It has been suggested that a possible explanation for the die drool phenomenon onset is the high value of negative pressure which can occur at the die exit region.[7] It has been found that for mLLDPE, the critical value of such pressure is −1.6 MPa. The main aim of this article is to explore in more depth the significance of negative pressure on the die drool phenomenon and specific attention will be paid to the effect of die design on this unwanted phenomenon.

Correspondence to: M. Zatloukal (mzatloukal@ft.utb.cz).
Contract grant sponsor: Ministry of Education CR; contract grant numbers: KONTAKT ME08090, MSM 7088352101.

EXPERIMENTAL

The experimental measurements were performed on 19 mm conventional Brabender single-screw extruder with a length $L = 25$ D equipped with a specially developed annular extrusion die (Fig. 1). The extrusion sections (from the hopper to the die) were heated to the following temperatures: $T_1 = 135°C$, $T_2 = 180°C$, $T_3 = 190°C$, $T_4 = 190°C$, whereas the annular tube between extruder and annular die was heated to the temperature $T_5 = 125°C$ only. The die wall temperature was 110°C and the die exit wall was cooled to 85°C with the help of cooling medium channel. At the fixed processing conditions (mass flow rate, temperature, etc.) the die exit geometry (described in Fig. 2) was varied to determine the stable/unstable conditions with respect to the die drool phenomenon.

During the experiments, a digital camera has been used to quantify the level of the die drool phenomenon at the die lip area. To quantify this, a die drool amount (DDA) variable has been proposed.

$$\mathrm{DDA} = \frac{A_D}{A_{\mathrm{Die}}} \frac{t_D}{t_{\mathrm{Die}}} \tag{1}$$

where A_D is area occupied by the die drooled material during the accumulation cycle, A_{Die} is the capillary die area, t_D is die drool accumulation time, and t_{Die} is time between die drool accumulation cycles, which is explained in greater detail later in this article. In this work, the mLLDPE Exact 0201 (octane-1 plastomer, metallocene type) has been used. The

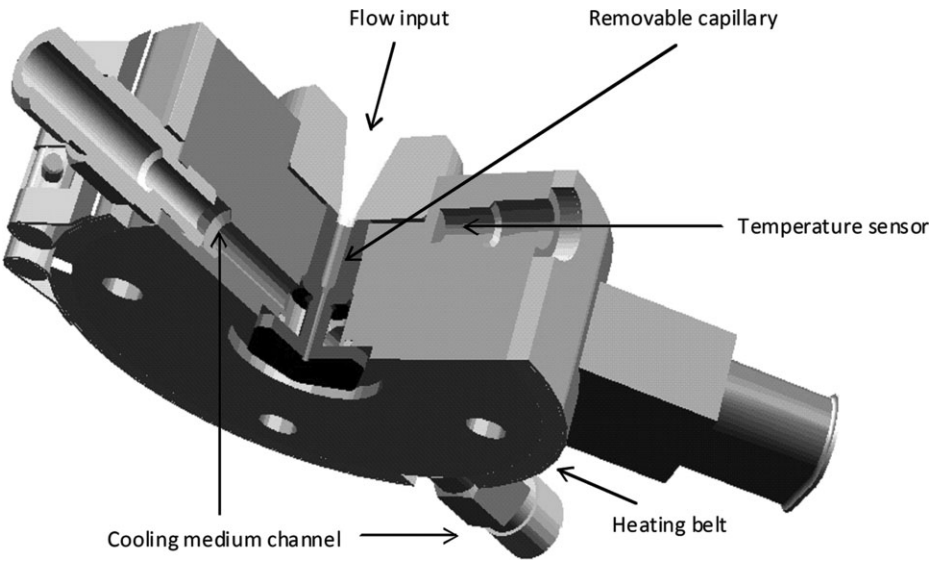

Figure 1 Annular extrusion die with internal cooling system for the die lip.

basic characteristics for this material are presented in Table I.

It should be mentioned that this indirect method is very useful for the evaluation of die drool intensity because of its potential applicability under weak die drool conditions, where direct DDA measurements is very difficult or impossible. Additionally, the use of indirect techniques significantly reduces possible errors arising from careless collection of accumulated material from the die lip area. The application of digital image analysis by using a single camera is limited only to the processing conditions where 3D effects can be neglected (such as drool thickness or drool rotation in 3D space leading to "different" 2D surface area for identical drool amount). For the material and processing conditions used in this work, the digital image analysis has been performed within 60 min to minimize this type of the error.

Figure 3 shows a typical mechanism of the die drool phenomenon observed during the extrusion of mLLDPE by using the experimental set-up described above. As can be seen, the die drooled material initially sticks to the die lip in form of small flakes and then the material accumulation increases to the point, that it is completely sheared from the die exit

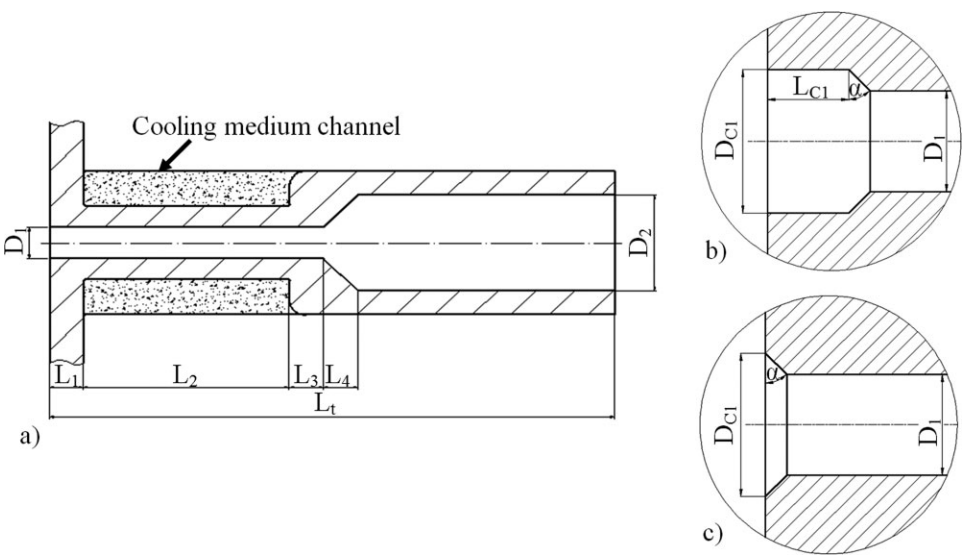

Figure 2 Detail description of the removable capillary $L_1 = 2$, $L_2 = 10$, $L_3 = 2$, $L_4 = 2$; $L_t = 33$, $D_2 = 6$: (a) Straight die (No. 1): $D_1 = 1.6$; (No. 2): $D_1 = 2$; (b) The detail of flared die (No. 3): $L_{C1} = 0.5$, $D_{C1} = 2$, $D_1 = 1.6$, $\alpha = 45°$; (c) The detail of shaped die (No. 4): $D_{C1} = 2$, $D_1 = 1.6$, $\alpha = 45°$; (No. 5): $D_{C1} = 2$, $D_1 = 1.6$, $\alpha = 15°$; (No. 6): $D_{C1} = 2.4$, $D_1 = 2$, $\alpha = 45°$; (No. 7): $D_{C1} = 2.8$, $D_1 = 2$, $\alpha = 45°$ (all dimensions are provided in mm).

TABLE I
The Basic Characteristics of the Tested mLLDPE Taken from Ref. 8

Material	Density (g/cm^3)	M_w (g/mol)	M_n (g/mol)	M_z (g/mol)	M_w/M_n
mLLDPE Exact 0201, Exxon	0.902	88700	41449	158900	2.140

surface by the moving extrudate. In this work, these three stages represent the "Die drool accumulation cycle" and the corresponding time for this cycle is called, t_D (die drool accumulation time). Under particular processing conditions, the die drool accumulation cycles may periodically repeat with a certain time delay between them, in which no die drool occurs. This time delay is called t_{Die} (time between die drool accumulation cycles).

MATHEMATICAL MODELING

Nonisothermal viscoelastic steady state two-dimensional finite element simulations were performed by solving the well-known mass, momentum and energy equations using the commercially available Compuplast software VEL 6.1. In this study, the modified White-Metzner (mWM) constitutive equation according to Barnes and Roberts[9] is employed. The nonisothermal mWM model is given by eqs. (2)–(5).

$$\tau + \lambda(\mathrm{II}_d)\overset{\nabla}{\tau} = 2\eta(\mathrm{II}_d)d \tag{2}$$

$$\eta(\mathrm{II}_d) = \frac{\eta_0 f}{[1 + (K_1 f \mathrm{II}_d)^a]^{(1-n)/a}} \tag{3}$$

$$\lambda(\mathrm{II}_d) = \frac{\lambda_0 f}{1 + K_2 f \mathrm{II}_d} \tag{4}$$

$$f = e^{\frac{E_a}{R}\left(\frac{1}{T} - \frac{1}{T_r}\right)} \tag{5}$$

where E_a is the activation energy, R is the gas constant, T_r is the reference temperature, T is the temperature, d is the rate of deformation tensor, II_d is the second invariant of the rate of deformation tensor, τ is the stress tensor, $\overset{\nabla}{\tau}$ is the upper convected time derivative of stress tensor. $\lambda(\mathrm{II}_d)$ is the deformation rate-dependent relaxation time and $\eta(\mathrm{II}_d)$ is the deformation rate-dependent viscosity, η_0 is zero shear-rate viscosity and λ_0, K_1, K_2, n, a are constants. The model parameters for the mLLDPE material used in this work are provided in Table II. Behavior of the mWM model for the tested mLLDPE is summarized in Figure 4 in terms of Trouton ratio, T_r, and recoverable shear, S_R, which are used to assess the viscoelastic character of the polymer melt in extensional and shear flow, respectively.

$$T_r = \frac{\eta_E}{\eta_S} \tag{6}$$

$$S_R = \frac{N_1}{2\tau_{\mathrm{xy}}} \tag{7}$$

where N_1 is the first normal stress difference, τ_{xy} is the shear stress, and η_E and η_S are extensional and shear viscosity, respectively. It should be noted that even if the mWM model behaves similarly to KBKZ or XPP models (see Refs. 10,11) in term of quantitative T_r prediction, the mWM model unrealistically predicts S_R value to be constant at higher shear rates (see Fig. 4). Boundary conditions and the corresponding FEM grid used to describe the flow in capillary die are shown in Figures 5 and 6, respectively.

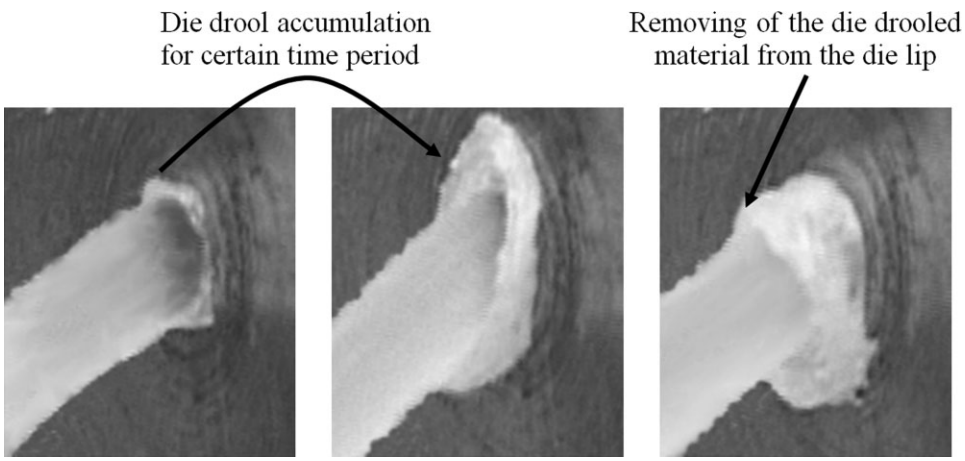

Figure 3 Die drool development during extrusion of mLLDPE (1 kg/h, 90°C) at the capillary die exit.

TABLE II
Fitting Parameters of the Modified White-Metzner Model for mLLDPE Taken from Ref. 7

Material	η_0 (Pa s)	n	K_1 (s)	a	λ_0 (s)	K_2 (s)	E_a (kJ/mol)	T_r (°C)
mLLDPE Exact 0201, Exxon	38469	0.1	0.0592	0.2795	7545	11956	41.023	170

The typical calculated pressure profile at the die exit region of a reference die with a sharp die exit corner (see Figure 2a, for more details) is depicted in Figure 7. It is clearly visible that negative pressure occurs in that region which has been proposed in our previous work as the one factor causing the die drool phenomenon.[7] Note that for the tested mLLDPE polymer and the chosen processing conditions, the wall shear rate in the analyzed flow domain varies from 0.1 1/s up to approximately 300 1/s, i.e., the recoverable shear is constant, equal to 0.63 (see Fig. 4).

It is interesting to investigate why the predicted die swell level depicted in Figures 6 and 7 for viscoelastic mWM (describing mLLDPE melt) is lower than that predicted for purely Newtonian fluids at low Reynolds numbers where extrudate diameter/capillary diameter ration is 1.13. The explanation is as follows: It is well known that at very low Reynolds number capillary flows, the die swell for Newtonian fluids (having an index of non-newtonian behavior equal to 1 and no elasticity) is caused by the amount of velocity rearrangement at the die exit region where the parabolic velocity profile, occurred in the die land, is change to be constant in the extrudate. On the other hand, if a shear thinning fluid is considered (having index of non-newtonian behavior equal to 0 and no elasticity) at very low Reynolds number capillary flows, the die swell disappears. This is because no velocity rearrangement occurs at the die exit region due to plug flow (constant velocity profile) occurrence in the die land region. Therefore, if the index of non-newtonian behavior decreases from 1 down to 0 for no elastic fluids in very low Reynolds numbers capillary flows, the die swell decreases from 13% down to 0%. As shown in Table II, the index of non-newtonian behavior of tested mLLDPE is only 0.1 and therefore the die swell due to velocity rearrangement at the die exit region is, in this case, very low. Additionally, due to the high shear thinning character of the mLLDPE, the elasticity predicted by the mWM model is very low (the maximum attainable recoverable shear, is

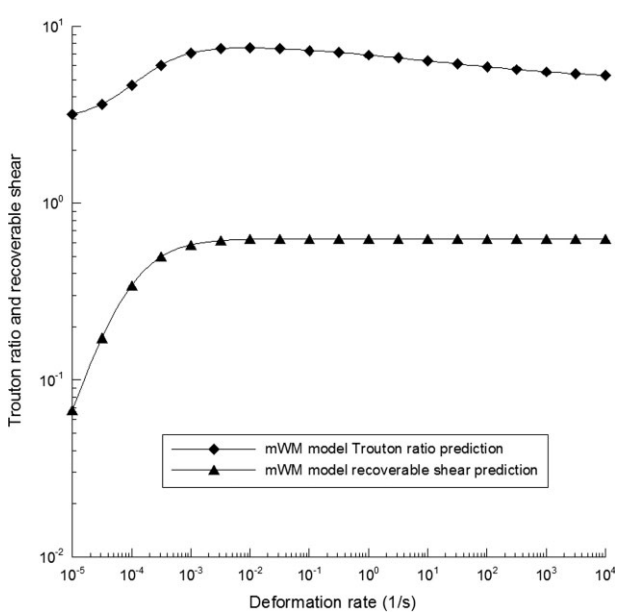

Figure 4 mWM model prediction of Trouton ratio (for uniaxial extensional flow) and recoverable shear for mLLDPE model parameters summarized in Table II.

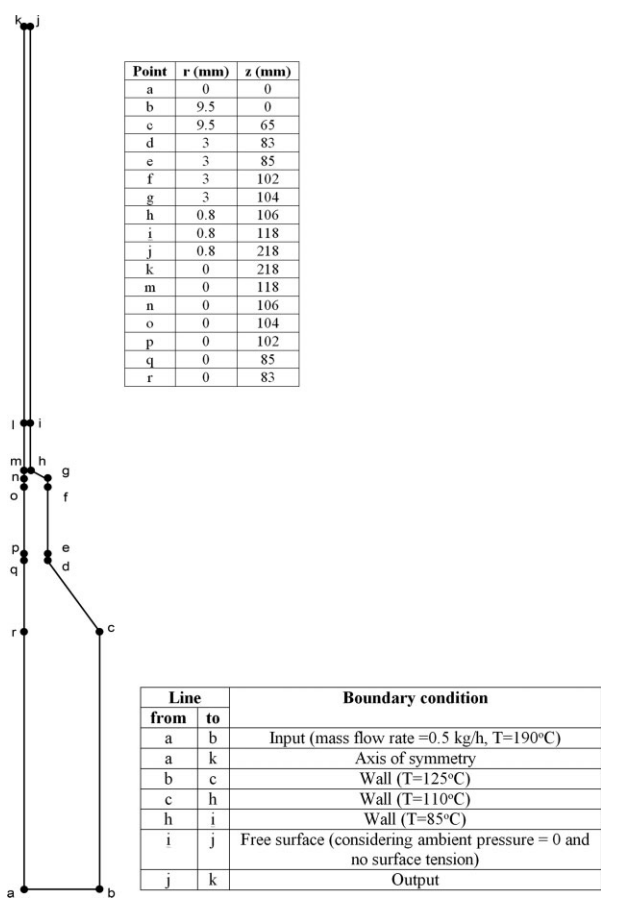

Point	r (mm)	z (mm)
a	0	0
b	9.5	0
c	9.5	65
d	3	83
e	3	85
f	3	102
g	3	104
h	0.8	106
i	0.8	118
j	0.8	218
k	0	218
m	0	118
n	0	106
o	0	104
p	0	102
q	0	85
r	0	83

Line		Boundary condition
from	to	
a	b	Input (mass flow rate =0.5 kg/h, T=190°C)
a	k	Axis of symmetry
b	c	Wall (T=125°C)
c	h	Wall (T=110°C)
h	i	Wall (T=85°C)
i	j	Free surface (considering ambient pressure = 0 and no surface tension)
j	k	Output

Figure 5 Boundary conditions used for die No. 2.

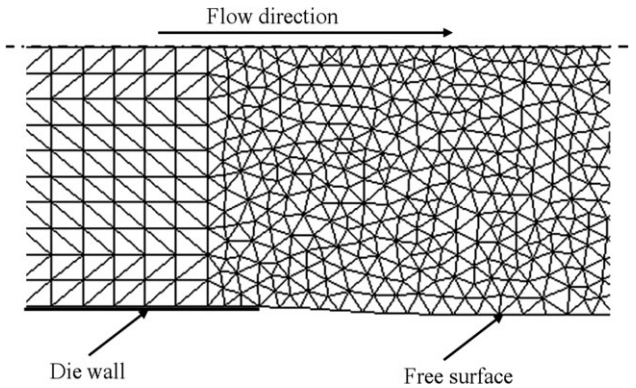

Figure 6 FEM grid used for the die exit modeling for die No. 2.

only 0.63—see Fig. 4) and thus it is insufficient to increase the die swell above 13% in this case.

In the next section, the negative pressure will be discussed in more detail with respect to experimental data and melt elasticity.

RESULTS AND DISCUSSION

The effect of die design

First, the effect of the die exit wall angle α on the DDA has been investigated experimentally and theoretically. The most important experimental data are visualized in Figure 8. It is clearly visible that the correct design of die exit geometry can suppress the die drool phenomenon significantly. The modification of the reference die [depicted on Fig. 2(a), die No. 1] has been found to decrease the DDA from 4.43 (predicted negative die exit pressure = −1.76 MPa) down to 0.15 by chamfering of the die exit wall under angle α = 15° [Fig. 2(c), die No. 5]. This represents a 96.6% reduction in die drool. Full die drool suppression has been achieved by chamfering the die exit wall under angle α = 45° [Fig. 2(c), die No. 4]. Note that the predicted negative die exit pressure has been found to be −1.27 MPa in this case. In both cases, the processing conditions were kept the same i.e., mass flow rate = 0.4 kg/h, die exit wall temperature 85°.

Second, the effect of completely different die designs (straight die No. 1, shaped die No. 4, flared die No. 3—see Fig. 2 for more details) on the die drool phenomenon has been investigated for different mass flow rates (0.3–1.3 kg/h) at one fixed die exit wall temperature (T = 85°C). The experimental data are depicted in Figure 9. As can be seen in these figures, the general trend of the DDA versus mass flow rate dependence for all three tested geometries takes nonmonotonic shape. The die deposit increases up to critical value of mass flow rate and then gradually decreases. An apparent decrease of the die drool level at higher flow rates is caused by intensively moving extrudate which almost continuously starts to remove the die drooled material from the die lip.[4,7] The experimental data in Figure 9 clearly shows that shaped die No. 4 and flared die No. 3 are highly effective in the die drool

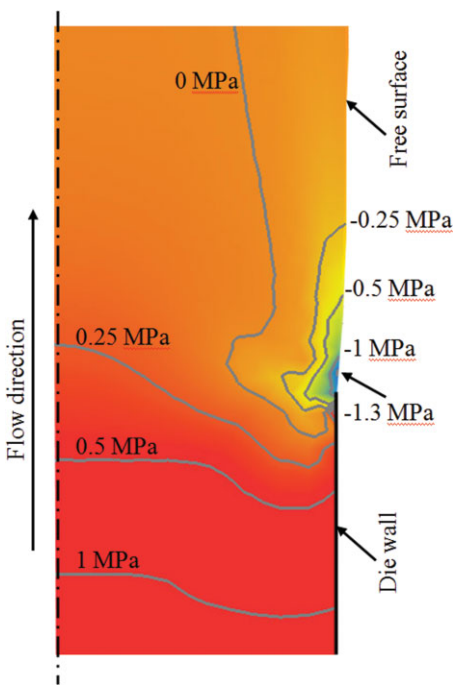

Figure 7 The predicted pressure field for the extrusion of mLLDPE (0.5 kg/h, 85°C, die No. 2). [Color figure can be viewed in the online issue, which is available at www.interscience.wiley.com.]

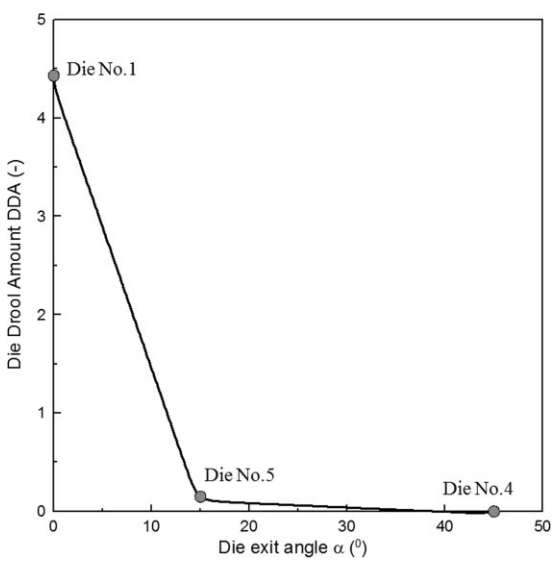

Figure 8 Effect of the die drool amount on the die exit angle α. The points represent measurements (0.4 kg/h, 85°C).

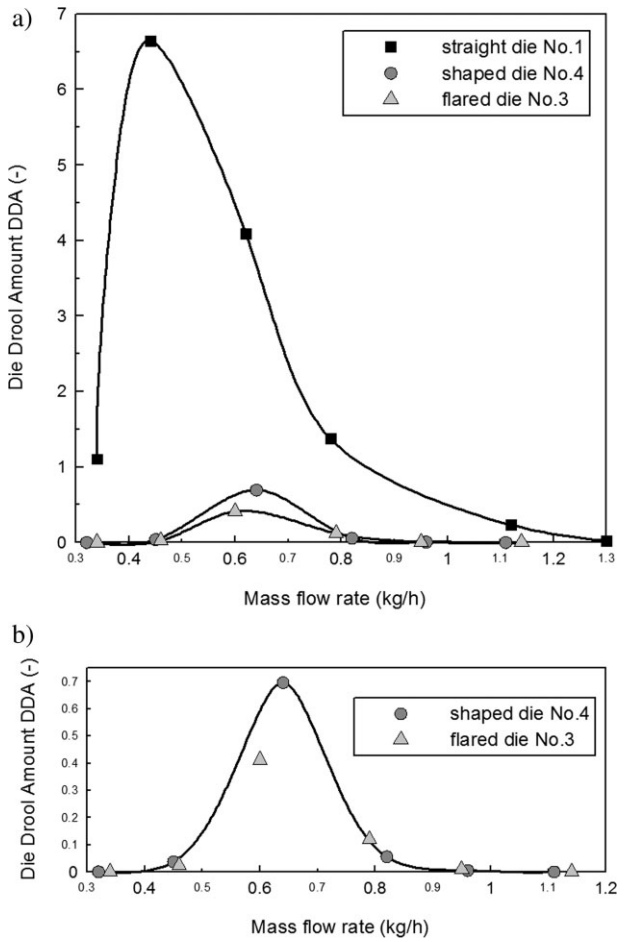

Figure 9 The effect of the mass flow rate and the shape of die exit geometry on the level of die drool (0.4 kg/h, 85°C). (a) Results for geometries No. 1, 3, and 4; (b) Detailed view for Geometries No. 3 and 4.

elimination compared to the reference straight die No. 1. The flared die No. 3 reduces die drool even more effectively than the shaped die No. 4. This conclusion is supported by the experimental work of F. Ding et al.[6] where it has been reported that flared geometry of the film blowing die lips can cause as much as 94% reduction of the die drool. Subsequently, the experimental data in Figure 9 have been followed by the viscoelastic FEM analyses of each experiment (with particular capillary die design) and the corresponding maximum negative pressure values occurring at the end of the die, were determined. The results of the FEM analysis are shown in Figure 10. It is clearly visible that the calculated values of the negative pressure at the die exit wall for all investigated dies were found to be in good agreement with experimentally determined stability trends shown in Figure 9, i.e., higher stability corresponds with lower values of negative pressure.

Finally, the effect of die exit opening geometry on the die drool phenomenon has been investigated for different mass flow rates (0.4–1.2 kg/h) at one fixed die exit wall temperature (T = 85°C). Two dies (shape die No. 6 and shape die No. 7) were considered as the special modifications of straight die No. 2, where abrupt corners were reduced to 45° on the 0.2 mm length—shape die No. 6, and 0.4 mm length—shape die No. 7 (see Fig. 2 for more details). The experimental data showing DDA for each die design and the processing conditions are depicted in Figure 11. Clearly, a higher level of the die exit opening (represented by the shape dies No. 6 and 7) leads to a much more pronounced reduction of the die drool phenomenon. Also in this case, the experiments were followed numerically and the maximum negative pressure was calculated for each particular case. The typical theoretical data are depicted in Figure 12. Even if the negative pressure is predicted correctly to be lower for a more stable case, the difference between straight die No. 2 and shape die No. 6 is unexpectedly predicted to be very small (see large differences between flow stability for straight die No. 2 and shape die No. 6 depicted in Figure 11). This finding suggests that the maximum negative pressure value itself may not be sensitive enough to accurately predict the die drool phenomena. Therefore, two additional variables (maximum pressure gradient and the normal component of the pressure gradient) were calculated for each particular processing condition and plotted in Figures 13 and 14. In these Figures, lower levels of the pressure gradient or its normal component correspond to more stable cases of die drool, i.e., the stability trends are correctly predicted with respect to Figure 11. It seems that in this particular case, these two variables can distinguish more precisely the stability

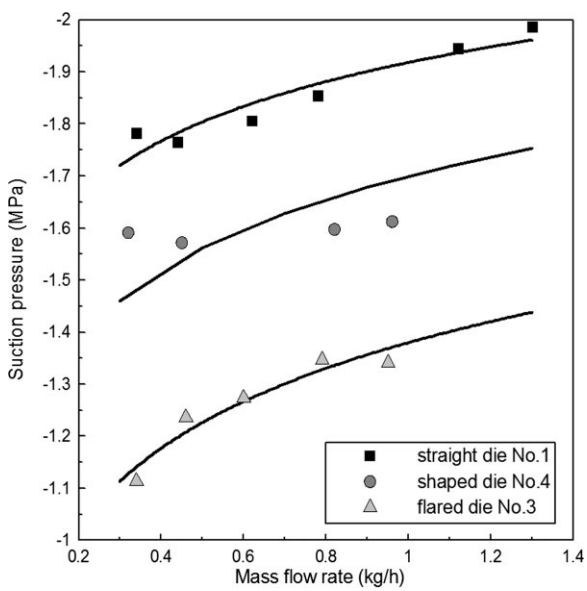

Figure 10 The predicted suction pressure as a function of the mass flow rate for tested geometries No. 1, 3, and 4 (0.4 kg/h, 85°C).

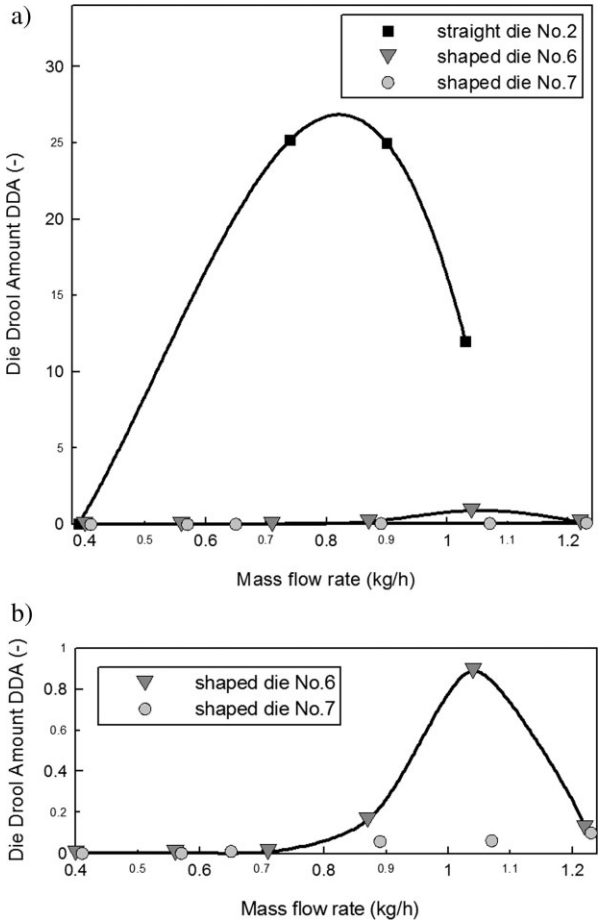

Figure 11 The effect of the distance of chamfering angle on die drool amount (0.4 kg/h, 85°C). (a) Results for geometries No. 2, 6, and 7; (b) Detailed view for Geometries No. 6 and 7.

differences between straight die No. 2 and shape die No. 6 than the maximum negative pressure value.

Significance of the negative pressure

The reasons for the negative pressure occurrence in the studied flow domain and its impact on the die drool phenomenon is now discussed here in more detail. In our previous work,[7] we have discussed that the so-called external die drool can be explained by the negative pressure occurring at the die exit region where the free surface of the extrudate is created. It is interesting to determine whether the negative pressure can also explain so-called internal die drool, i.e., flow induced fractionation occurring inside the die, and what is the role of melt elasticity in this case. To determine these two relationships we have investigated theoretically the effect of melt elasticity on the pressure profile inside the virtual die having the diverging die exit region (with no free surface region) with both a smooth transition at the top wall and a sharp transition at the bottom wall

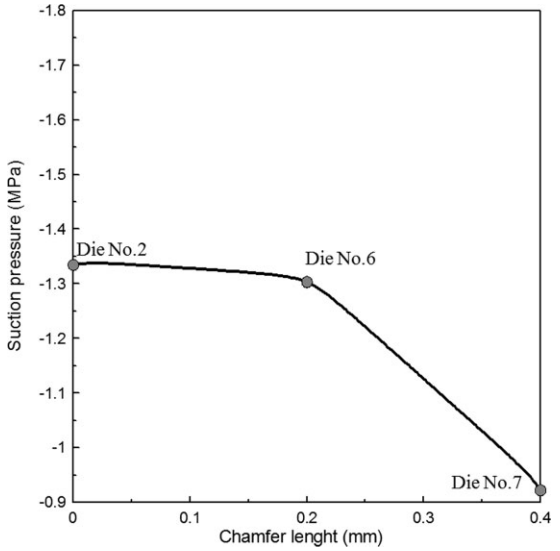

Figure 12 The effect of the distance of chamfering angle on suction pressure (0.5 kg/h, 85°C).

(see Fig. 15). Figure 16(a) shows the pressure profiles, for elastic mLLDPE polymer melts, along the top (top wall detail in Fig. 15) and bottom wall (bottom wall detail in Fig. 15). It is clearly visible that first, negative pressure may occurs inside the die and second, the higher value of the negative pressure corresponds to the sharp transition. This suggests that possible separation of low molecular weight components/fillers from the viscoelastic polymer melt matrix may also occur inside the dies. This can contribute to the higher accumulation level at the die exit wall. Figure 16(b) shows practically the same results as in the Figure 16(a) but with a nonelastic mLLDPE polymer melt (in this case, the

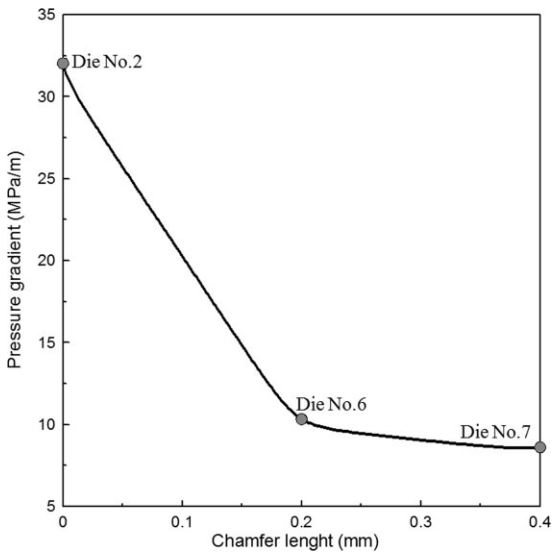

Figure 13 The effect of the distance of chamfering angle on pressure gradient (0.5 kg/h, 85°C).

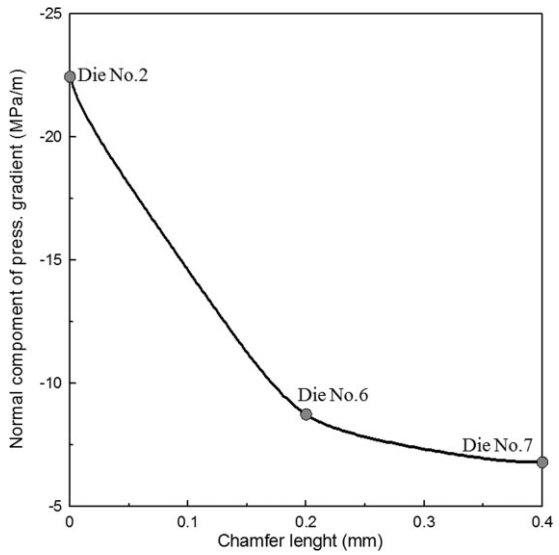

Figure 14 The effect of the distance of chamfering angle on normal component of pressure gradient (0.5 kg/h, 85°C).

relaxation time λ_0 in eq. (4) is equal to zero, which causes the transition of the viscoelastic mWM model into the simple generalized Newtonian law with no elasticity). It is clearly visible from comparison between Figure 16(a,b) that a decrease in the melt elasticity significantly reduces negative pressure occurrence inside the die. With the aim to quantify the internal/external die drool phenomenon as much as possible from the theoretical point of view, the magnitude of the pressure gradient, defined by eq. (8), might also be considered because this variable is very sensitive to the abrupt change in the pressure profile which usually occurs at the pressure profile minimum or maximum.

$$\overline{\nabla p} = \sqrt{\left(\frac{\partial p}{\partial t}\right)^2 + \left(\frac{\partial p}{\partial n}\right)^2} \tag{8}$$

It should be noted that $\overline{\nabla p}$ is calculated according to eq. (8) by using a local (streamline) coordinate

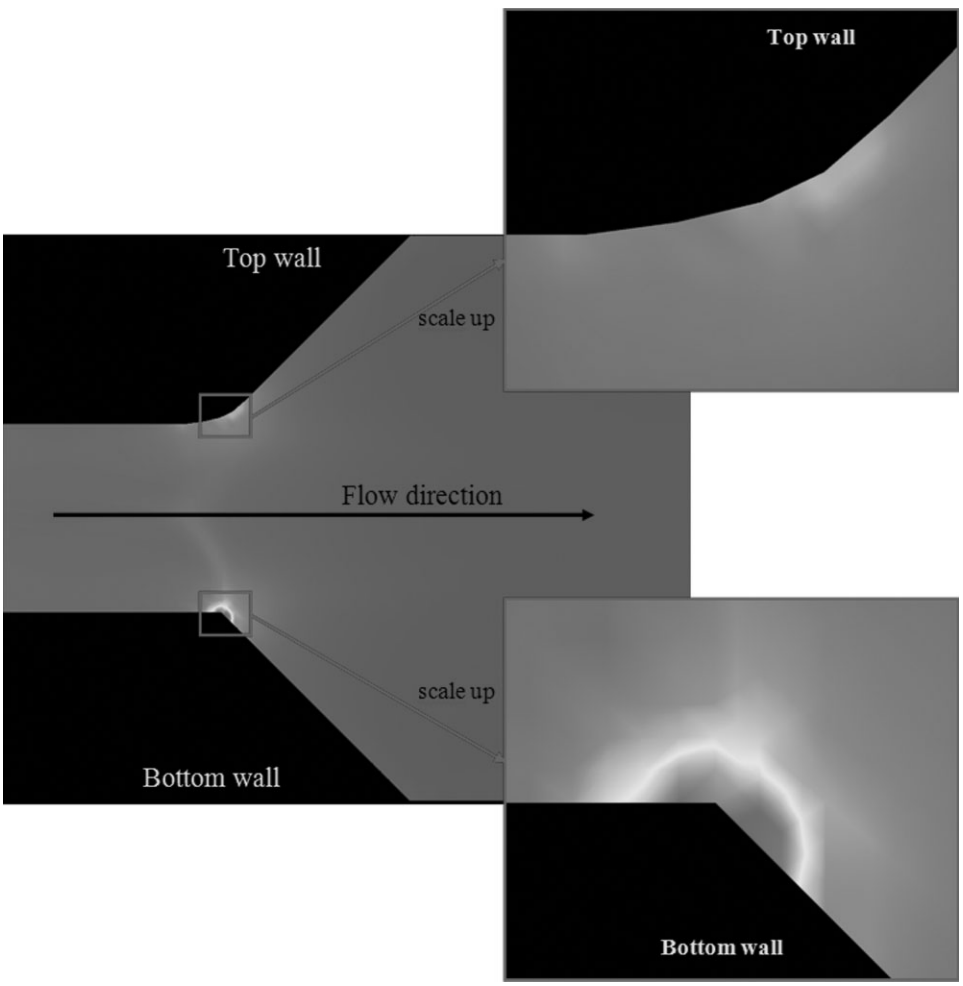

Figure 15 Flow of the viscoelastic melt inside the virtual extrusion die having diverging exit region with smooth (upper wall) and sharp (bottom wall) transition. Predicted pressure gradient magnitude field. Red and blue represents high and low pressure gradient magnitude value, respectively.

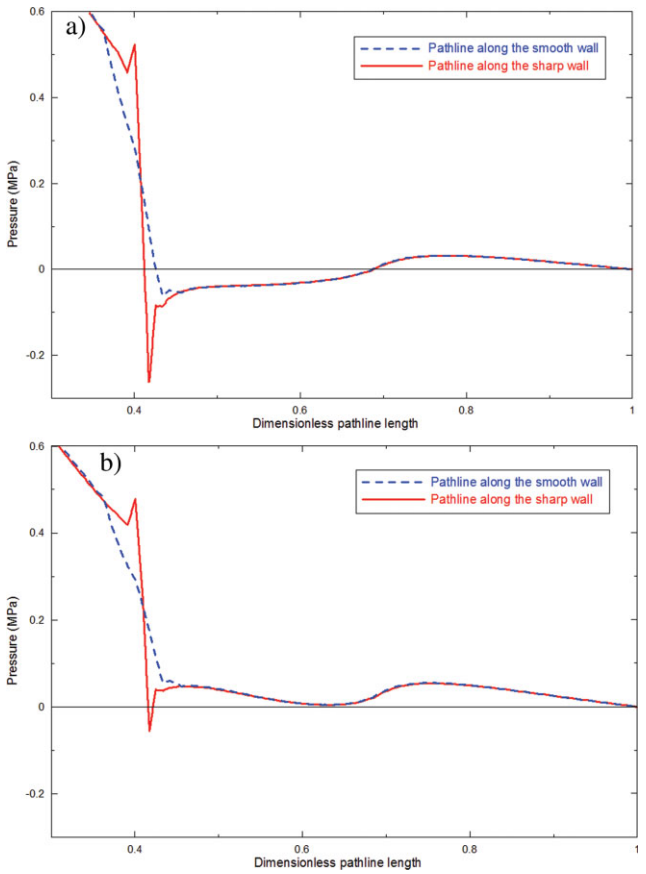

Figure 16 Calculated pressure profile (for two chosen pathlines) during the melt flow in the virtual extrusion die depicted in the Figure 13. (a) viscoelastic mLLDPE melt—model parameters are provided in Table II; (b) no elastic mLLDPE melt—model parameters are provided in Table II but relaxation time has been adjusted to be $\lambda_0 = 0$, i.e., $\lambda(II_d)$ in eq. (4). [Color figure can be viewed in the online issue, which is available at www.interscience.wiley.com.]

system where t and n represent tangential and normal directions to the flow direction, respectively.

If the pressure gradient magnitude field (Fig. 15) is compared with the principle stress difference (PSD) field for studied virtual die (Fig. 17) we can see that sensitivity of the $\overline{\nabla p}$ to the transition smoothness into the diverging channel is much higher than in the case of the PSD. Finally, the normal component of the pressure gradient $\partial p/\partial n$ can also be useful in helping to understand the die drool phenomena because it quantifies the possible separation force occurring during melt elasticity or poor die design, in the normal direction (toward the die wall) with respect to the flow direction. Therefore, the use of the pressure, $\overline{\nabla p}$, and $\partial p/\partial n$ with respect to the internal/external die drool phenomena is recommended.

There remain the following questions which must be addressed with respect to the issue of negative pressure.

1. May the Newtonian fluid such as water possess negative pressure at the die exit region? This is possible because Newtonian fluids may also have negative pressure since in the free surface $\tau_{nn} - p = 0$, i.e., as the Newtonian fluid is leaving the die, velocity rearrangement from parabolic to constant velocity profile occurs. This leads to the stretching of the Newtonian fluid in the tangential direction close to the free surface (τ_{tt} has a positive sign) whereas compression occurs in the normal direction (τ_{nn} has a negative sign). Therefore, the stress at the free surface is only $\tau_{nn} - p = 0$ if the pressure p is negative. Since polymer melts are viscoelastic and have memory, high viscosity and Trouton ratio, absolute values of $-\tau_{nn}$ and $-p$ are much higher compared with the Newtonian fluids.
2. Can the die drool phenomenon be present during Newtonian flow? In general, die drool is a spontaneous accumulation of material at the die lip. In the case of a polymer melt, the viscosity of the accumulated material is reasonably high and material accumulation takes place within the extrusion time because gravity induced sag does not usually occur. In the case of a Newtonian fluid such as water, the accumulated material at the die exit sags immediately due to the low liquid viscosity and it can be seen that the face of the tube exit is wetted. This can also be viewed as a special case of the die drool phenomenon and negative pressure can be a factor promoting this.
3. Why was the pressure rather than stress state at the die exit region used for the die drool

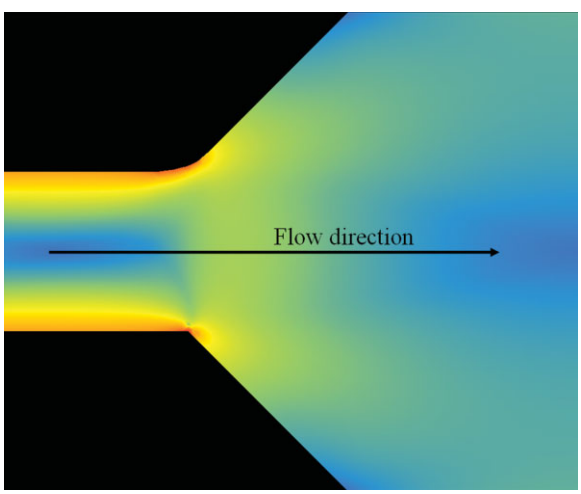

Figure 17 Flow of the viscoelastic melt inside the virtual extrusion die having diverging exit region with smooth (upper wall) and sharp (bottom wall) transition. Predicted principle stress difference field. Red and blue represents high and low principle stress difference value, respectively. [Color figure can be viewed in the online issue, which is available at www.interscience.wiley.com.]

analysis in this work? To explore this point in more detail, it is necessary to clarify the effect of pressure in the flowing viscoelastic liquid (see recent articles by Dealy[12] and Han[13] for useful discussions). In most polymer processing flows, the deformation leads to anisotropy of the normal stresses and pressure as the scalar variable has no unique definition. In this case, suitable constitutive equations together with the mass, momentum and energy conservation laws have to be solved to determine the pressure. Therefore, the pressure can be viewed as the simple scalar variable helping us to understand the way in which viscoelastic polymer melts isotropically compensate shear and internal anisotropic normal stress rises due to imposed flow deformation history in the normal 3D space directions. Considering this the pressure can be understood to be a very useful and simple variable for theoretical analysis since it provides valuable information regarding the mechanism in which the stress is compensated during the flow. Because of the fact that die drool phenomenon is the consequence of the specific type of the polymer melt stress increase compensation occurring during flow, the pressure rather than stress has been utilized in this work. It should be mentioned that Tremblay,[14] by using isothermal finite element analysis employing generalized Newtonian fluid, also obtained and discussed negative pressure at the die exit region. In his work, by using negative pressure only, the polymer melt fracture at the die exit (well known as the shark skin phenomenon) has been explained.

Based on the discussion above, it is believed that variables such as pressure, pressure gradient and the normal component of the pressure gradient can be used to understand stabilizing/destabilizing factors during polymer processing, especially, relating to the die drool phenomena.

CONCLUDING REMARKS

- It has been determined experimentally that chamfering of the die exit wall under angle $\alpha = 15–45^\circ$, opening the die or the use of a flared die significantly reduces the die drool phenomenon.
- It has been speculated that internal die drool can be explained by negative pressure inside the die.
- It has been suggested that pressure, magnitude of the pressure gradient and normal pressure gradient components can be useful variables for theoretical investigation of the die drool phenomenon.

The authors thank Dr. Jiri Vlcek, Dr. Jiri Svabik, and Dr. Ilja Paseka from Compuplast International, for very useful discussion about the negative/nonmonotonic pressure profile interpretation.

References

1. Gander, J. D.; Giacomin, A. J. Polym Eng Sci 1997, 37, 1113.
2. Dhori, P. K.; Jeyaseelan, R. S.; Giacomin, A. J.; Slattery, J. C. J Non-Newtonian Fluid Mech 1997, 71, 231.
3. Lee, Ch. D. SPE ANTEC Tech Papers 2002, 48, 264.
4. Chai, K. C.; Adams, G.; Frame, J. SPE ANTEC Tech Papers 2001, 47, 401.
5. Chan, C. M. Intern Polym Proc 1995, 3, 200.
6. Ding, F.; Zhao, L.; Giacomin, A. J.; Gander, J. D. Polym Eng Sci 2000, 40, 2113.
7. Chaloupkova, K.; Zatloukal, M. Polym Eng Sci 2007, 47, 871.
8. Pivokonsky, R.; Zatloukal, M.; Filip, P. J Non-Newtonian Fluid Mech 2008, 150, 56.
9. Barnes, H. A.; Roberts, G. P. J Non-Newtonian Fluid Mech 1992, 44, 113.
10. Mitsoulias, E.; Schwetz, M.; Munstedt, H. J Non-Newtonian Fluid Mech 2003, 111, 41.
11. Pivokonsky, R.; Zatloukal, M.; Filip, P.; Tzoganakis, C. J Non-Newtonian Fluid Mech 2008; doi:10.1016/j.jnnfm.2008.06.001.
12. Dealy, J. M. Rheol Bull 2008, 77, 10.
13. Han, C. D. Polym Eng Sci 2008, 48, 1126.
14. Tremblay, B. J Rheol 1991, 35, 985.